Proceedings of the Indian National Science Academy (2026) 92:1056–1069
https://doi.org/10.1007/s43538-025-00445-8

RESEARCH PAPER

Investigation effect of arterial stenosis on shear stress and blood flow characteristics: computational fluid dynamics study

Nan Tang[1,2] · Kangming Li[1,2] · Haoran Li[1] · Chunmei Qi[1]

Received: 7 August 2023 / Accepted: 28 April 2025 / Published online: 4 June 2025
© Indian National Science Academy 2025

Abstract
Occlusion of the coronary arteries is one of the most important causes of death and permanent complications in the body. Stiffening of the vessel wall or atherosclerosis is the main cause of clogged arteries. Therefore, the objective of the current research was to investigate the influence of coronary artery stenosis on blood flow to the arteriole of the heart through physical modeling. In the present research, the effect of stenosis in the coronary artery was studied, assuming two types of platelets: cubic and cylindrical. The modeling and analysis were done using computational fluid dynamics (CFD) simulations. Blood was considered a non-Newtonian fluid, and the hypotheses of a fully developed area at the vessel entrance were used. Then, the influence of different parameters, such as platelet type and the presence of stents, on the characteristics of intravascular blood flow, including pressure distribution, shear stress, and blood velocity, was studied. The results show that the type of platelets and the presence of stents have a significant effect on the characteristics of intravenous blood flow. The maximum pressure created in a stent with a cube-shaped platelet and cylindrical platelets is 180 Pa and 172 Pa, respectively, and the maximum pressure in the case of cylindrical platelets is about 5% less than the presence of a cubic platelet. Furthermore, due to the higher amount of shear stress in the cube-shaped platelet artery, it can be said that the occurrence of this clogging in the vessel has much more serious risks and the risk of cardiovascular disease increases.

Keywords Arteriole of the heart · Arteriole stenosis · CFD analysis · Blood flow · Shear stress

Introduction

Mathematical models have a very significant role in the field of medicine. In medicine, decisions are traditionally based on population research, the medical history of the patient, and the experiences of the doctor. These factors are considered in determining the most appropriate treatment for each patient. Recently, mathematical models based on physical laws have proved to be a very valuable and reliable resource for doctors. The use of simulation software and computational methods such as the finite element method and computational fluid dynamics (CFD) will be useful in investigating the structural-fluid interaction of heart performance (Malinauskas et al. 2017). Developing a computational model that accounts for the geometry and anatomy of an artery the mechanical properties of vessel tissue, and investigating structure-fluid interaction using the built-in models can prove to be a valuable tool for medical applications (Bluestein et al. 2013). Hence, it is essential for providing CFD simulations of clogged arteries (Suzuki et al. 2020; Wells and Marvin 2021).

Fluid flow into different ducts has been studied by many researchers using analytical and numerical methods (Rezaee and Arab Maleki 2012, 2017, 2019; Eslami et al. 2016; Rezaee and Maleki 2015). Peskin (1977) proposed a new model with focused parameters for cardiovascular dynamics. Van Loon et al. (2006) investigated the model of fluid–solid interaction with solid–solid contact for heart valves. This composition is especially vital for studying the dynamics as well as heart rate of the valves. Taylor et al. (2013) investigated the fluid–solid interaction simulation in the aortic valves. In their study, two finite element models have been used to study the interaction of fluid flow with aortic valve function. A three-dimensional pattern of the left

✉ Chunmei Qi
760020220858@xzhmu.edu.cn

[1] Department of Cardiology, Second Affiliated Hospital of Xuzhou Medical University, Xuzhou 221000, Jiangsu, China

[2] Graduate School of Xuzhou Medical University, Xuzhou 221000, Jiangsu, China

ventricle with wall displacement to generate data was used for the spatiotemporal profile of velocity in the aortic valve. Wigmond et al. (2008) investigated the impact of bundle branch closure on cardiac outputs. According to the study, the heart is controlled electronically by the fluid pump that works by mechanical contractions. Li et al. (2018) evaluated the simulation of blood flow in a flexible clogged artery. In this study, non-permanent blood flow and the performance of arterial walls were modeled for the true geometry of the abdominal aorta and leg branches in different positions. Blood is assumed to be non-Newtonian, incompressible, and viscous, and the solid wall tissue is homogeneous, elastic, and isotropic. Some work treats blood as Newtonian flow (Fraser et al. 2012), and some treat it as Non-Newtonian (Li et al. 2020).

In general, simulation, when done correctly, can be the main method of recognizing and analyzing any real phenomenon. Nowadays, the science of simulation is used in a variety of fields (Sadeqi et al. 2021; Fatholahi et al. 2021; Maghami et al. 2021; Nabavi et al. 2021a, 2021b). For example, medical engineering has tools that allow the simulation of biological phenomena inside the human body. Studies using CFD techniques to simulate left ventricular blood flow have each been representative of the true model of the left ventricle. In the study of Long et al. (2008), while creating a simple geometric model for the left ventricle to model the mitral valve, an oval platelet with an area of three square centimeters was used for all phases. In their study, fluid flow was performed using ANSYS CFX and considering blood as a Newtonian fluid via constant viscosity and incompressible. Due to the fact that experimental methods are invasive methods and it is not possible to create laboratory conditions for prediction in most cases, numerical simulation has been used as a useful tool to understand this more accurately (Zhao et al. 2021; Skopalik et al. 2021).

The presence of clogging in the blood vessels increases the shear stress (SS), which causes the inner wall of the arteries to thicken and increases the amount of clogging due to the separation of blood from the wall. Using CFD simulations, Kot and Abbas (2017) examined a hard-walled, symmetrically occluded blood vessel. In their study, the equations governing the speed of blood flow, the stresses on the vessel wall, and how red blood cells pass in two normal states with the attendance of clots have been studied. Devi and Vijaya (2017) investigated the nanofluid flow of blood inside clogged coronary arteries. Prasad et al. (2017) studied the impact of occlusion of the branching carotid artery of the neck on blood flow features, such as shear stress of the wall, using ANSIS-Fluent software. Blood flow is considered smooth, incompressible, stable, Newtonian, and rigid, and the constant pressure difference between the outer and inner sides of the vessel is considered. They considered the vessel once without clogging and again with 75% clogging and the results of the two cases were compared with each other, and the validation of the results was checked. The results showed that clogging reduces the inlet flow rate and increases the shear stress of the vessel wall. Leng et al. (2017) numerically examined the nanofluid flow of blood inside the clogged coronary arteries. Kamada et al. (2017) examined the pulsed flow of blood in narrowed ducts using non-Newtonian fluid and Newtonian for parabolic clogging. Bidel et al. (2014) investigated the relationship between risk factors and coronary artery stenosis in patients referred to the angiography center in Mehran. Using CFD, Bahadori et al. (2017) investigated a hard-walled blood vessel with symmetrical occlusion. Zang et al. (2018) performed a simulation of blood flow and hemodynamic parameters in a carotid artery with a porous and flexible double-walled wall using a finite element solution for porous fluid–solid interaction. Liu et al. (2018) numerically studied the mass transfer of low-density lipoproteins in the primary part of the cerebral carotid artery called the common carotid artery. For this purpose, numerical modeling of blood flow and mass transfer of lipoprotein particles in an artery with a four-layer wall has been studied. Navier–Stokes equations and mass transfer in the arterial canal area and flow and mass transfer equations related to the porous body were used to simulate the processes. In the study, Zhu et al. (2019) investigated the instability of blood flow due to small blockages in the vessel wall that are on the verge of formation and growth. Blood flow is modeled as a Newtonian pulsed fluid flow in a two-dimensional channel with local occlusion. Moshfegh et al. (2018) investigated the biomechanical damage to the pulsed blood flow in a clogged artery using ADINA software. To solve the turbulent flow, the K-ε RNG turbulence model was used, which was better adapted to the laboratory work compared to the numerical work of other K-ε Standard models and was better able to show the return flow region. Nejad et al. (2018) simulated the pulsed fluid flow of intravenous blood that has clogged and the effect of clogging geometry and physical features of the patient's vessel on the physical characteristics of blood flow and vessel wall in the presence of the clogged vessel were reported.

As mentioned, coronary artery occlusion is one of the most important causes of death and permanent complications in the body. Stiffening of the vessel wall or atherosclerosis is the main cause of stenosis arteries. Hence, the aim of this study was to evaluate the influence of stenosis severity on the vessel wall and also the presence of coronary artery occlusion on the blood flow to the arterioles of the heart through physical modeling. Furthermore, in recent years, the use of artery-opening devices such as stents to relieve clogged arteries has developed a lot. When using a stent, a cubic narrowing is created in the

vessel, so the effect of this type of narrowing and stenosis on the blood flow characteristics and hemodynamics has been studied for the first time in this study. In this study, an attempt was made to investigate the effect of the presence of congestion in the coronary artery on the flow characteristics of the lower arm and identify areas prone to congestion in the presence of congestion in the coronary artery. Real geometry and boundary conditions are used for modeling, and the commercial CFD software, Fluent software, was applied to simulate the flow flows in the arterial stenosis. Blood will be assumed to be non-Newtonian fluid, and the effect of two types of cube-shaped and cylindrical clogging on flow parameters will be studied.

CFD modelling

Fluid flow equations

The arbitrary Lagrangian–Eulerian (ALE) Navier–Stokes equations are used, which are obtained by substituting the relative velocity for the velocity transfer terms in the original velocity equation. The integral form of the Navier–Stokes equation (Durst 2008):

$$\frac{d}{dt}\int_{\forall}\rho d\forall + \int_{s}\rho\left(v - v_s\right).nds = 0. \tag{1}$$

$$\frac{d}{dt}\int_{\forall}\rho v d\forall + \int_{s}(\rho v\left(v - v_s\right) + pI - \tau).nds = 0, \tag{2}$$

where v is the fluid velocity, v_s is border velocity, s is the control volume, n represents the perpendicular to the surface of the fluid boundary, p is pressure, I is the identity tensor, and τ is the deviatoric stress tensor.

Non-Newtonian fluid model of blood

Some of the different models for simulating blood flow are:

- Blood can be described as a Newtonian fluid (Fraser et al. 2012).
- Consider non-Newtonian fluid blood and use a power model (Mandal et al. 2007).
- Let blood as a non-Newtonian fluid and use the Carreau model (Akbar and Nadeem 2014).

If blood is regarded to be a non-Newtonian fluid and modeled via the power law model, we will have (Husain et al. 2013):

$$\begin{aligned}&\rho = 1050\,\mathrm{kg/m^3};\ (\dot{\gamma}) = K\dot{\gamma}^{(n-1)};\\ &n = 0.7755; K = 0.01467\ \mathrm{mPa\ s};\end{aligned} \tag{3}$$

where n is the power law model index, and K is the compatibility index. For substances that have a thinning property, such as blood, the value of n is less than one.

Modeling a clogged vessel

A red blood vessel with a diameter of 6 mm and a length of 11 cm was used to measure the blood's movement and clots in partially clogged arteries. Figure 1 shows an example of the actual model of a clogged vessel with a stent.

Two kinds of clogging with cylindrical and cubic platelets are explored to examine the impacts of clogging. An artery that is clogged is supposed to have a symmetrical clog at a space of four centimeters from its entrance. The basic model of a clogged vessel and the stent is developed using Solidworks software and imported to ANSYS software. Figures 2 and 3 show an example of clogged vessel and stent geometry.

The blood vessel model (with dimensions), including its stenosis, is shown in Fig. 2 as a three-dimensional straight tube for numerical blood flow analysis. The cosine function defines the geometry of stenosis for cylindrical clogging as follows:

$$\frac{r(x)}{R} = 1 - \delta\left[1 + \cos(\pi x/D)\right], \quad -D \le x < D \tag{4}$$

x and $r(x)$ are the axial and radial coordinates, respectively. R and D represent the radius and diameter of un-stenosed arteries, respectively. δ is a constant and takes the values of 0.2 and 0.4, resulting in 30% and 60% diameter reduction at the stenosis throat, as displayed in Fig. 2.

The geometric model of the stand is shown in Fig. 3a. The focus of the present study is to investigate the effects of stents on the characteristics of intravenous blood flow. Therefore, using the non-slip boundary condition on the surfaces, CFD analyses are performed by placing the stent in a clogged artery. Figure 3b, c show the geometric model of the clogged vessels in the presence of the stand.

Plasma cells make up 56% of the blood, while blood cells make up 45%. Both plasma cells and blood cells have different densities, with plasma cells having a density of 1012 kg/m^3 and blood cells having a density of 1105 kg/m^3. A density value of 1050 kg/m^3 was used in the present study for whole blood. In the absence of slippage on the boundary walls and the non-movability of the boundary walls, the velocity in the wall is supposed to be negligible (Hariharan et al. 2015). A zero relative pressure was then specified at the domain outlet, and a fully developed velocity profile was specified at the inlet. Solvent types are selected based on pressure when performing an analysis. A volume control method is used in this study to discretize the flow equations, and the SIMPLE algorithm is used to solve them. For the infiltration sentences, the central

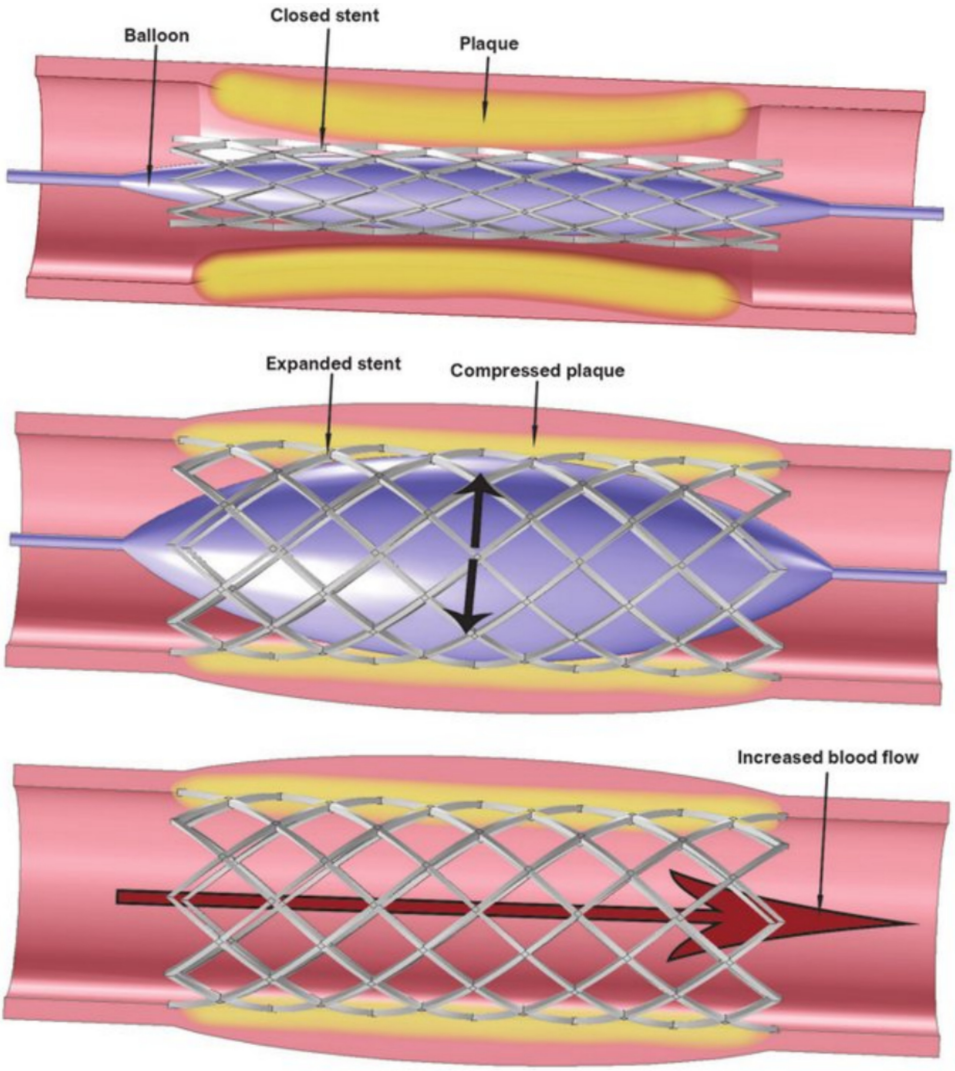


Fig. 1 A real model of a clogged vessel with a stent (Gudino et al. 2017)

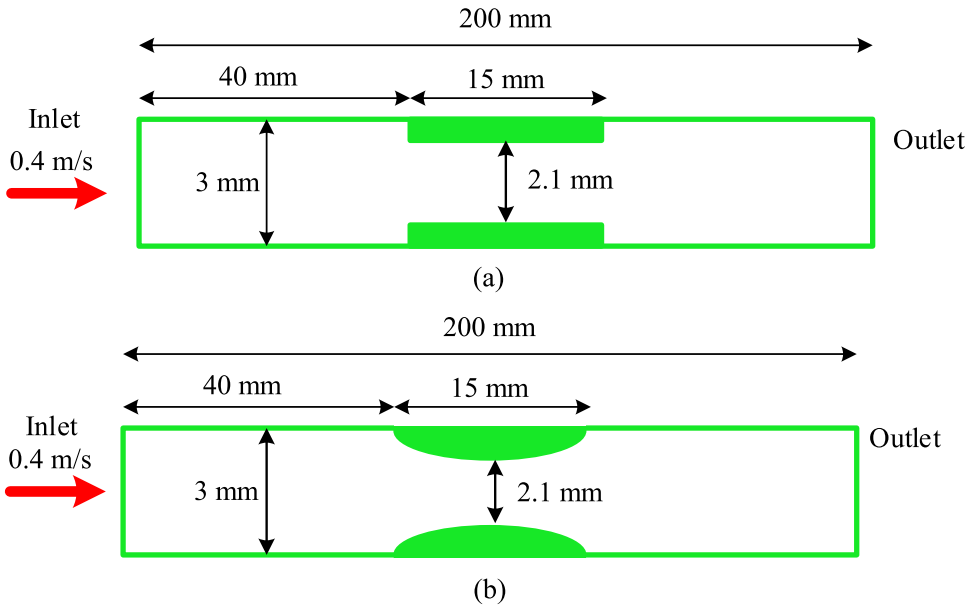


Fig. 2 Mathematical model of blood flows through an arteriole with stenosis **a** cubic stenosis geometry and **b** cylindrical stenosis geometry

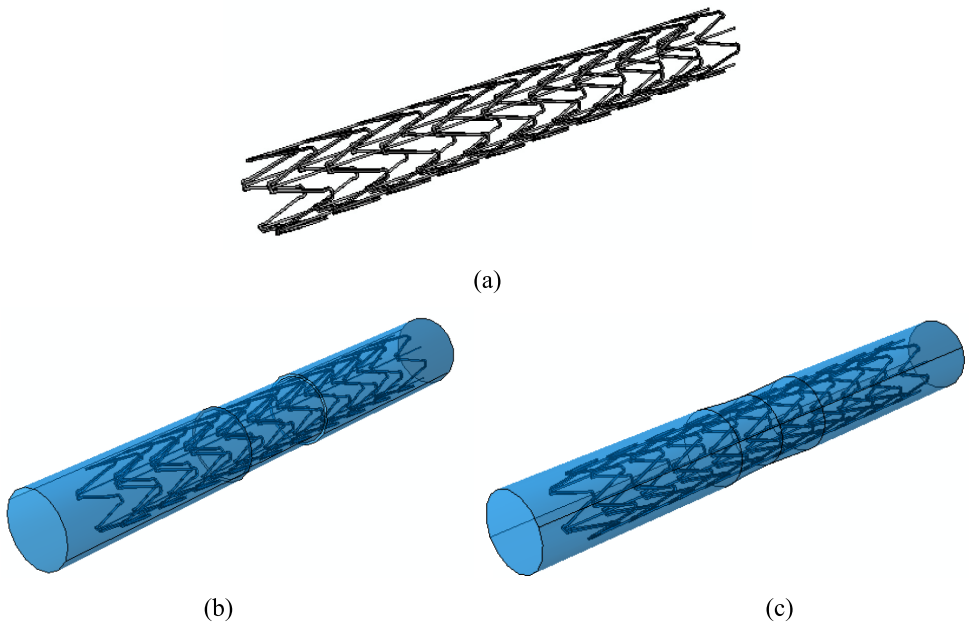


Fig. 3 **a** An actual stent used in CFD simulation, **b** cubic stenosis geometry with stent, and **c** cylindrical stenosis geometry with stent

difference approximation is used in the discretization of the equations. During the displacement sentence approximation, the hybrid approximation is applied, as well as the central difference approximation is used for the pressure sentence approximation. A sub-release coefficient for the velocity and pressure are 0.66 and 0.34, respectively, and a convergence criterion is taken into account for each component of velocity 10e−8 and pressure 10e−6. Tetrahedral elements were used for meshing. A mesh independence investigation was performed before determining the maximum element size used in this study to eliminate the potential effect of maximal element size on the CFD simulation outcomes. The numerical simulation is considered to be a steady-state solution since blood flow in an arteriole is quasi-steady and most articles consider blood flow to be steady. Because if the blood flow in the blood vessels is supposed to be unsteady flow, the human body experiences different states during the day and night. Furthermore, Steady-state flow simulations can provide information about the average behavior of blood flow over time. This information is still useful for understanding the overall hemodynamics and identifying potential issues or abnormalities. It is important to note that while steady-state simulations have their advantages, they may not capture certain transient or dynamic phenomena accurately. Therefore, it is essential to consider the limitations and assumptions made when interpreting the results and drawing conclusions from steady-state simulations.

Boundary condition

In this research, the boundary condition of the input speed with a fully developed profile is used at the entrance of the vessel equal to 0.4 m/s. The outflow with constant static pressure and no-slip boundary conditions were employed to outlet and wall boundary conditions, respectively. Also, the output distance from the end of the block is 40 mm, and the block length is 15 mm. Therefore, the output area is approximately ten times the length of the clogging, so the clogging has no effect on the output, and the condition of the developed current in the output can be used. In addition, the slip boundary condition is used in the walls. Also, due to the separate diameter at the inlet, the house is assumed to be a non-Newtonian and incompressible fluid. The bird-Carreau model has been used to model the non-Newtonian performance of blood. In this model, the viscosity limit at high and low shear rates is defined by constants. According to this model, fluid viscosity is defined as follows (Bai 2015):

$$\mu = \mu_0 + (\mu_0 - \mu_\infty)(1 + A\gamma^2)^n, \tag{5}$$

where $A = 10.976$, $\mu_\infty = 0.0035\,\text{Pa s}$, $\mu_0 = 0.056\,\text{Pa s}$ and $n = -0.3216$. Of course, this shear rate is completely higher than the accepted rate. Cho and Kensey (1991) have also stated that this model is in good consistency with experimental data.

Results

This paper discusses the results of CFD analyses performed on vessels with cylindrical as well as cubic platelets in which stents are placed. In the prior part, we described how to model using ANSYS software with border conditions, blood, and entry speed properties. In this section, we look at how the

parameters of intravenous blood flow are affected by the presence of clogging and the kind of clogging.

Convergence and mesh independence study

In determining whether the solution is independent of the network, the objective is to find the largest network that could accurately simulate the desired function (e.g., shear strain rate). Thus, the accuracy of the solution is completely dependent upon the network structure and mesh size. A simulation becomes more computationally intensive and time-consuming as the number of network cells increases. Performing simulations using a large-scale network is the first step in assessing the independence of the solution from the network. The desired outcome (like shear strain) is recorded after the solution convergence under these conditions. In the context of mesh independence from the network, the desired outcome is a parameter to be compared among various meshing sizes. Figure 4 shows an example of the method of checking the cube-shaped platelets' solution independence without using a stent. The shear strain results converged to 200 by raising the number of elements from roughly 0.7 million. As a result, this number of elements is employed in the analysis of the current study.

Effect of the stent

To investigate the influence of stents on the characteristics of intravenous blood flow, the condition of vessels with cylindrical platelets is first assessed. Figure 5 illustrates a comparison of pressure distributions in a vessel with a cylindrical platelet in two states with and without the presence of a stent. The results of this investigation show that the presence of stents has a significant influence on the distribution of pressure

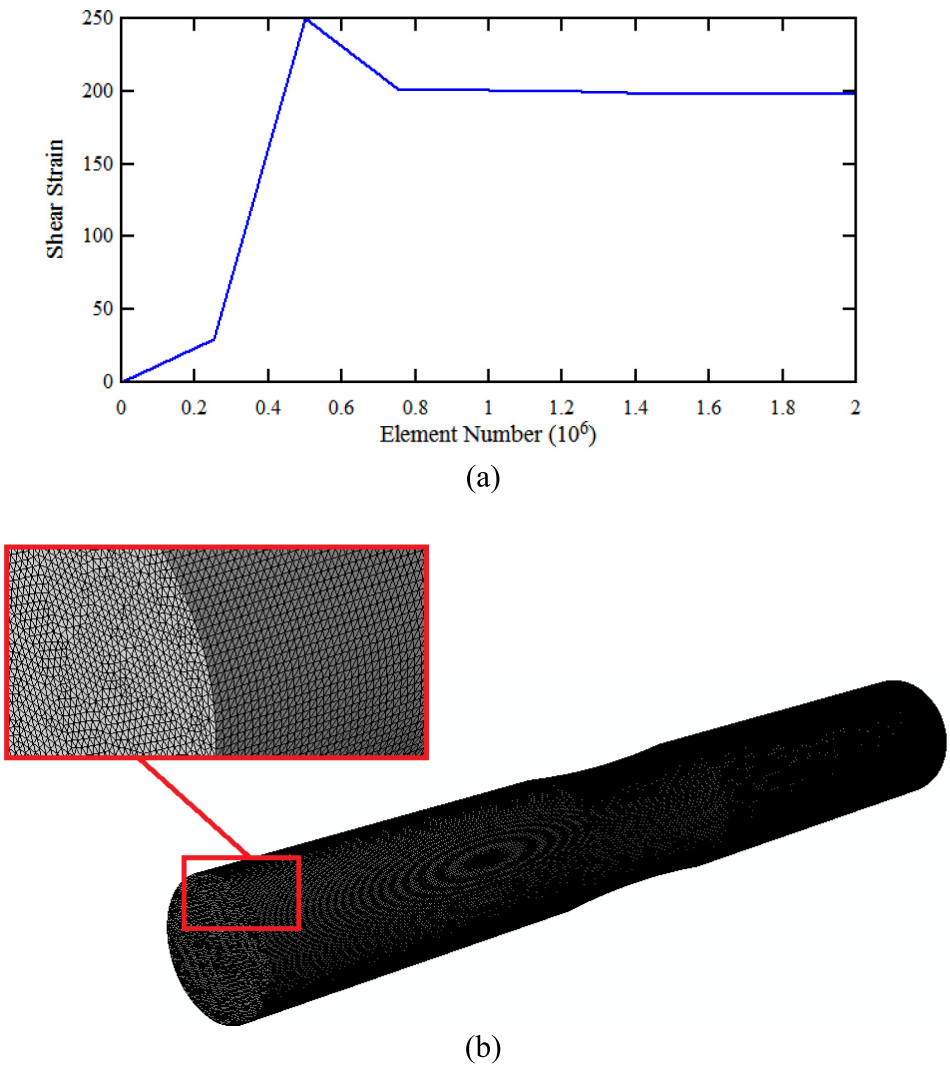


Fig. 4 **a** Mesh independence investigation for a cube-shaped plate without a stent and **b** CFD model and meshes for the vessel with cylindrical platelets

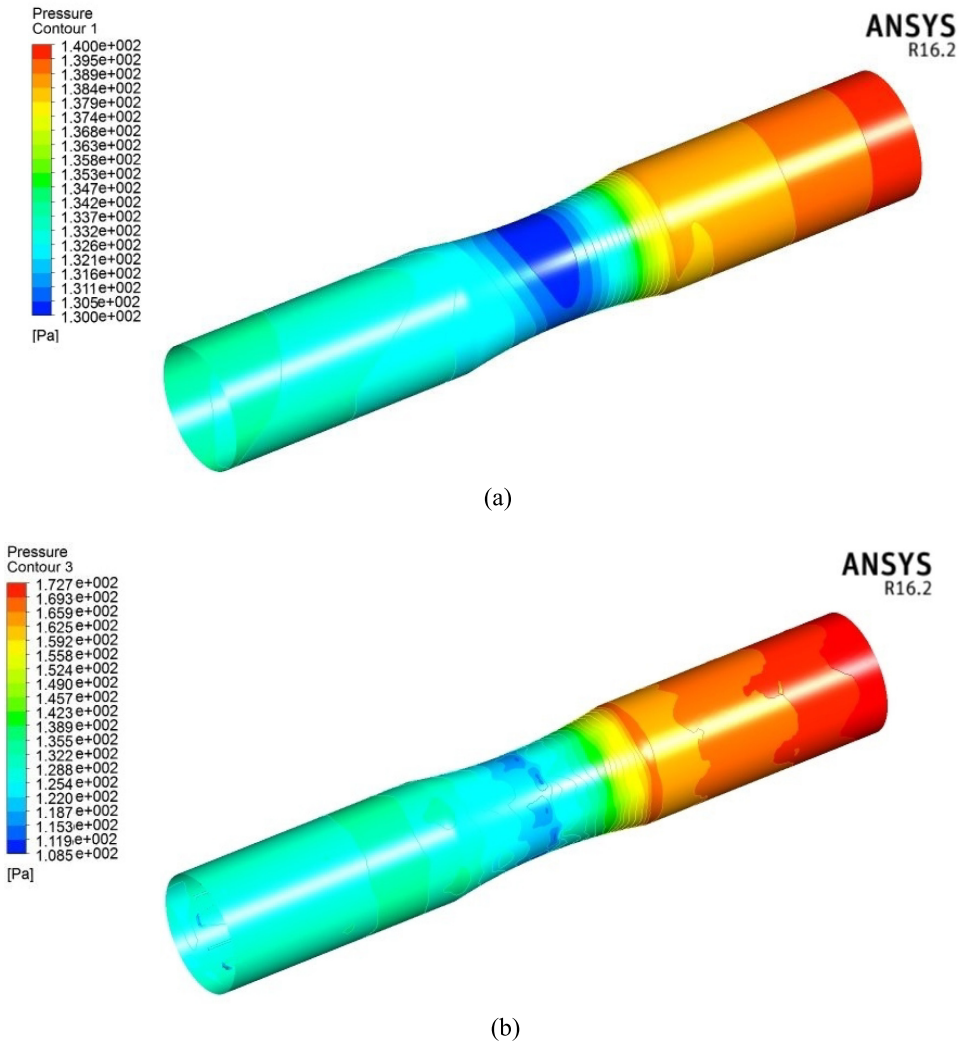


Fig. 5 Effect of a stent on the pressure distribution in a vessel with cylindrical platelets without stent and **b** with stent

within vessels. The maximum pressure created in a vessel with platelets in the presence of stents and the absence of stents averaged 140 Pa and 172.7 Pa, respectively. According to these results, stent implanting leads to an increase of 26% in the maximum pressure inside the vessel, which should be considered when using stents on patients. By implanting the stent in the vessel, the high-speed fluxes are increased in number and magnitude. As a result, the pressure drop in coronary arteries with stents is less than that of vessels without stents. Stent implantation can prevent the reduction of flow loss associated with arterial clogging, which leads to a decrease in pressure and flow after the clogging site.

The effect of platelet type

The impact of platelet kind on the feature of intravenous blood flow is determined. Figure 6 shows the pressure distribution for the vessel in two forms, plate-shaped, cube-shaped, and cylindrical, in the absence of stent use. According to the equation, it can be seen that the pressure at the beginning of the vessel has the highest value, and this maximum value continues until near stenosis. There is the greatest decrease in pressure in the stenosis, and after passing through the stenosis, its amount gradually increases. The maximum pressure for a cube and cylindrical platelet vessel is 180 Pa and 140 Pa, respectively. These results show that the maximum pressure in the cylindrical platelet state is about 28% lower than the maximum cubic platelet pressure.

In the following, the results of pressure distribution in a stented vessel with two types of cube-shaped and cylinder platelets are studied and displayed in Fig. 7. According to the outcomes, it can be seen that the maximum pressure is lower in the presence of cylindrical platelets, which is due to the gradual decrease in the lateral area of the vessel compared to the presence of cubic platelets in which the lateral area of the vessel suddenly decreases. The maximum tension created in

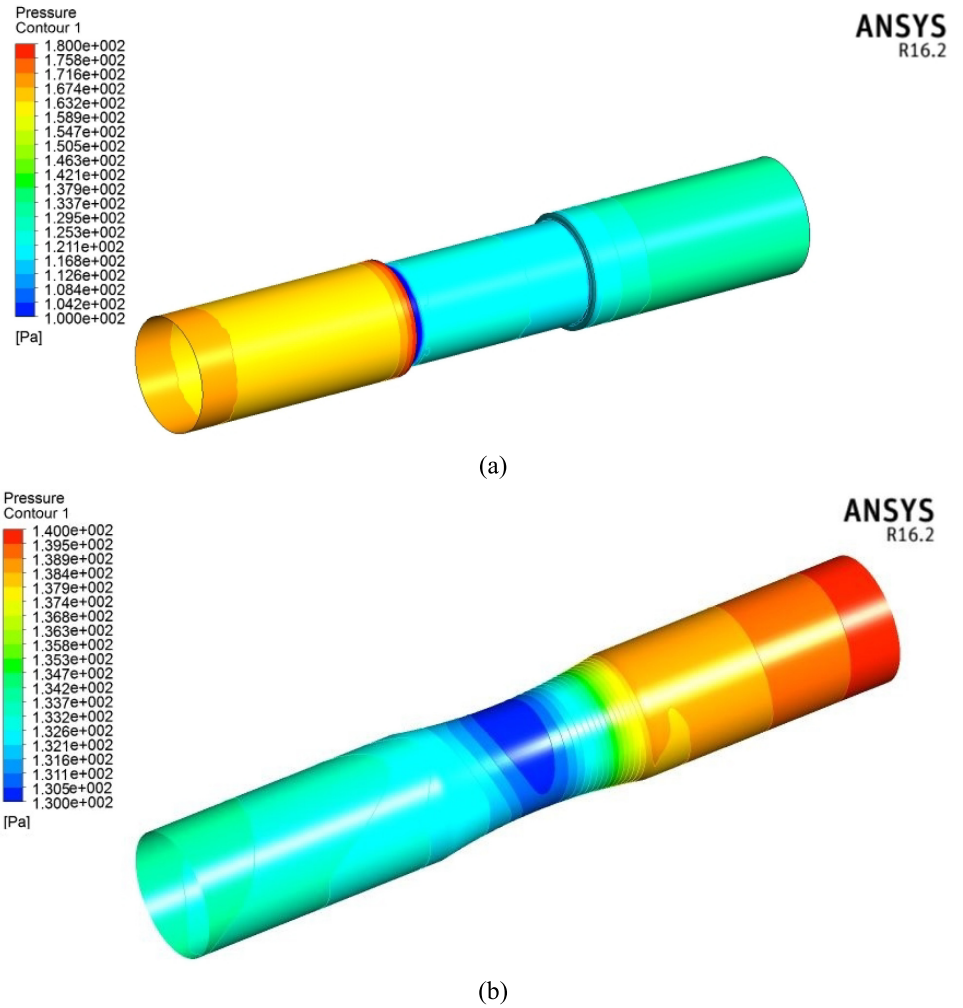


Fig. 6 Pressure distribution for a vessel in two states **a** cube-shaped platelets and **b** cylindrical platelets in the absence of the stent

the vessel increases. The results show that the maximum pressure created in the vessel with a stent with a cube-shaped plate and cylindrical plate is 180 Pa and 172 Pa, respectively, and that the maximum pressure in the case of a cylindrical plate is about 5% less than the presence of a cube plate.

Another important parameter in a vessel with platelets is the shear stress, which can cause the vessel to rupture if the amount is higher. Figure 8 shows the shear stress distribution for a vessel without a stent in cubic and cylindrical platelets. As the results show, platelet type shows the main impact on the shear stress distribution as well as its maximum value. In a cube-shaped plate with cylindrical platelets, the maximum shear stress is 7 Pa and 1.5 Pa, respectively, as the maximum shear stress in a vessel with cubic platelets is about 78% higher than in a vessel with cylindrical platelets.

Examination of shear stress distribution in vessels with cubic and cylindrical platelets shows that the distribution of shear stress in vessels with cubic platelets is more critical, and in most areas before vessel occlusion, the shear stress is maximum. According to Fig. 8, it is seen that the shear stress first excess at the site of the blockage, which occurs due to the increase in velocity at the site of the blockage, and after passing through the blockage, since the decrease in flow velocity behind the blockage, the shear stress also decreases. It should be noted that with the change of the type of clogging, the way of shear stress changes, and in the case of cylindrical plate-shaped vessels, due to the gradual change of blood velocity, the shear stress is less. It should be noted that increasing the shear stress causes the vessel to deform and increase in diameter, so increasing the diameter of the vessel and the passage of large volumes of blood is not only very effective on the mechanism of mass transfer but can also cause shock in the body. Shear stress due to damage to the endothelial layer changes in penetration and mass deposition inside the vessel can be considered a factor in the formation of fat plaques and an important factor in the development

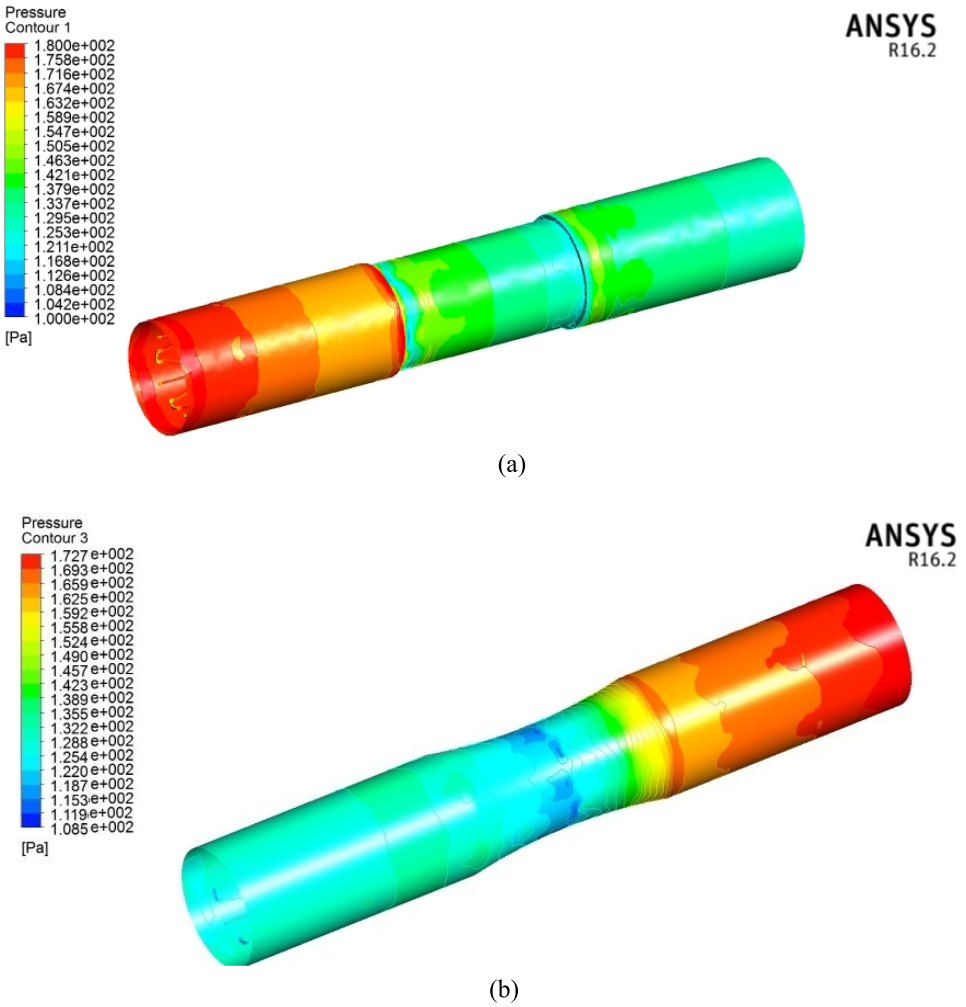


Fig. 7 Pressure distribution in a vessel with a stent **a** cubic platelets and **b** cylindrical platelets

of heart disease. Therefore, note the higher amount of shear stress in the cube-shaped plate artery. It can be said that the occurrence of this clogging in the vessel has much more serious risks and the risk of cardiovascular disease increases. Figure 9 depicts the effect of using a stent on the shear stress distribution in a vessel. Comparing these results with the results shown in Figs. 5, 6 and 7, it can be seen that although the use of stents does not cause any change in the maximum shear stress, it has a nominate impact on the distribution of SS. The results show that if a stent is used, areas with maximum shear stress are transferred to the site of vessel occlusion, and in these areas, the highest amount of shear stress occurs. These findings show that the maximum shear stress for the vessel with cubic platelets and cylindrical platelets is 7MPa and 1.5MPa, respectively, which indicates that in the presence of cubic platelets in the vessel, the maximum shear stress increases by about 78%. This outcome indicates that the clogged artery in the form of a cubic platelet is critical, which can cause the vessel to rupture.

Next, the velocity distribution of the fluid in the vessel is studied. Figure 10 indicates the velocity distribution of blood in a stent-bearing vessel in two forms: platelet-shaped and cylindrical platelets. The results show that the maximum blood velocity in the vessel with cubic plate and cylindrical platelets is equal to 0.4 and 0.46 m/s, respectively. It is more and, as a result, is less likely to cause cardiovascular disease in this condition.

Conclusion

To examine the impact of clogged arteries on blood flow characteristics, CFD analysis on clogged vessels was studied. In this study, blood was simulated as a non-Newtonian fluid, and the effect of two types of platelets, cubic and cylindrical, along with the use of stents on the pressure distribution as well as shear stress, were investigated. The key findings can be summed up as follows:

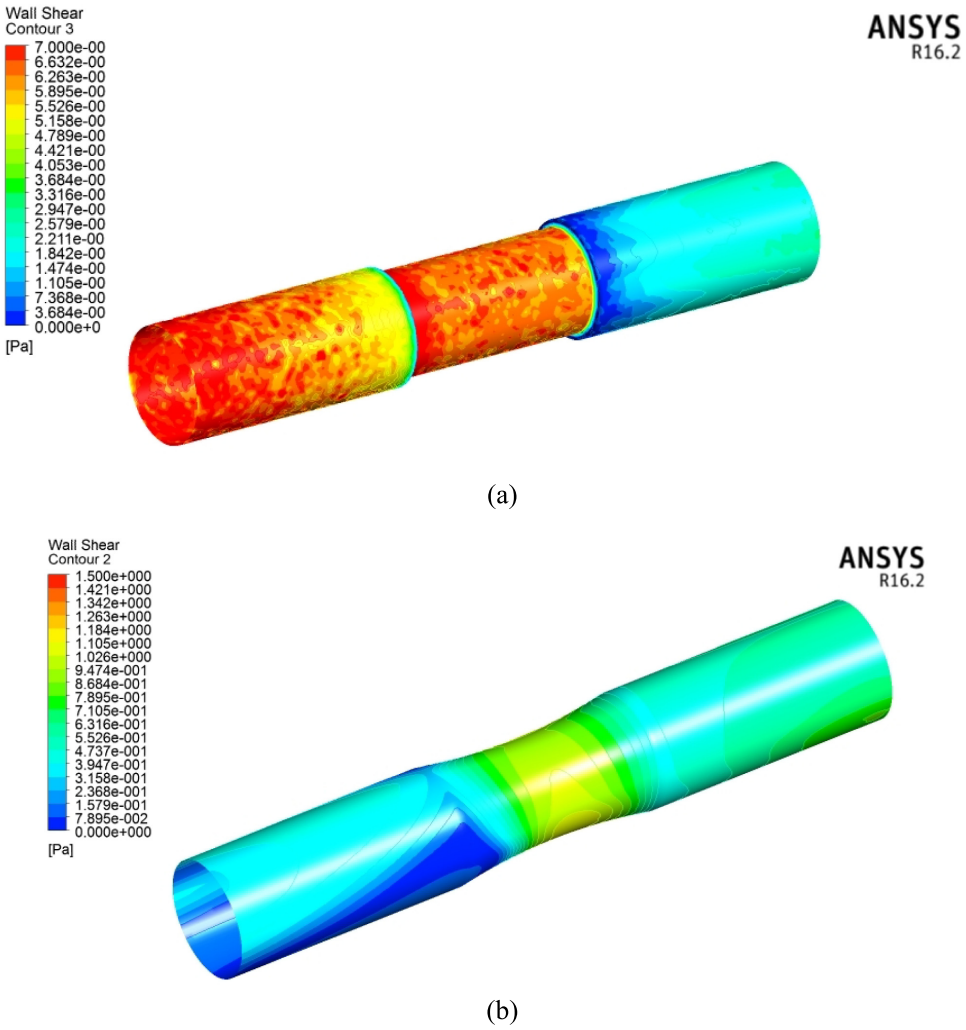


Fig. 8 Distribution of shear stress in the absence of stents for platelets with **a** cubic and **b** cylindrical geometry

- According to the findings, it can be seen that the pressure at the beginning of the vessel has the highest value, and this maximum value continues until near the throat. There is the greatest decrease in pressure in the throat, and after passing through the throat, its amount gradually increases.
- The maximum amount of pressure for a vessel with cubic platelets and cylinders without stents is 180 Pa and 140 Pa, respectively. These results show that the maximum pressure in the cylindrical platelet state is about 28% lower than the maximum cubic platelet pressure. The results show that the maximum pressure created in the vessel has a stent with a cube-shaped plate and cylindrical plate is 180 Pa and 172 Pa, respectively. The maximum pressure in the case of a cylindrical plate is about 5% less than the presence of a cube plate.
- The results show that platelet type shows a dominant impact on the distribution of shear stress as well as its maximum value. In a cube-shaped plate with cylindrical platelets, the maximum shear stress is 7 Pa and 1.5 Pa, respectively. Although the use of stents does not cause any change in the maximum shear stress, it shows a dominant impact on how the shear stress is distributed. The results show that if a stent is used, areas with maximum shear stress are transferred to the site of vessel occlusion, and in these areas, the highest amount of shear stress occurs.

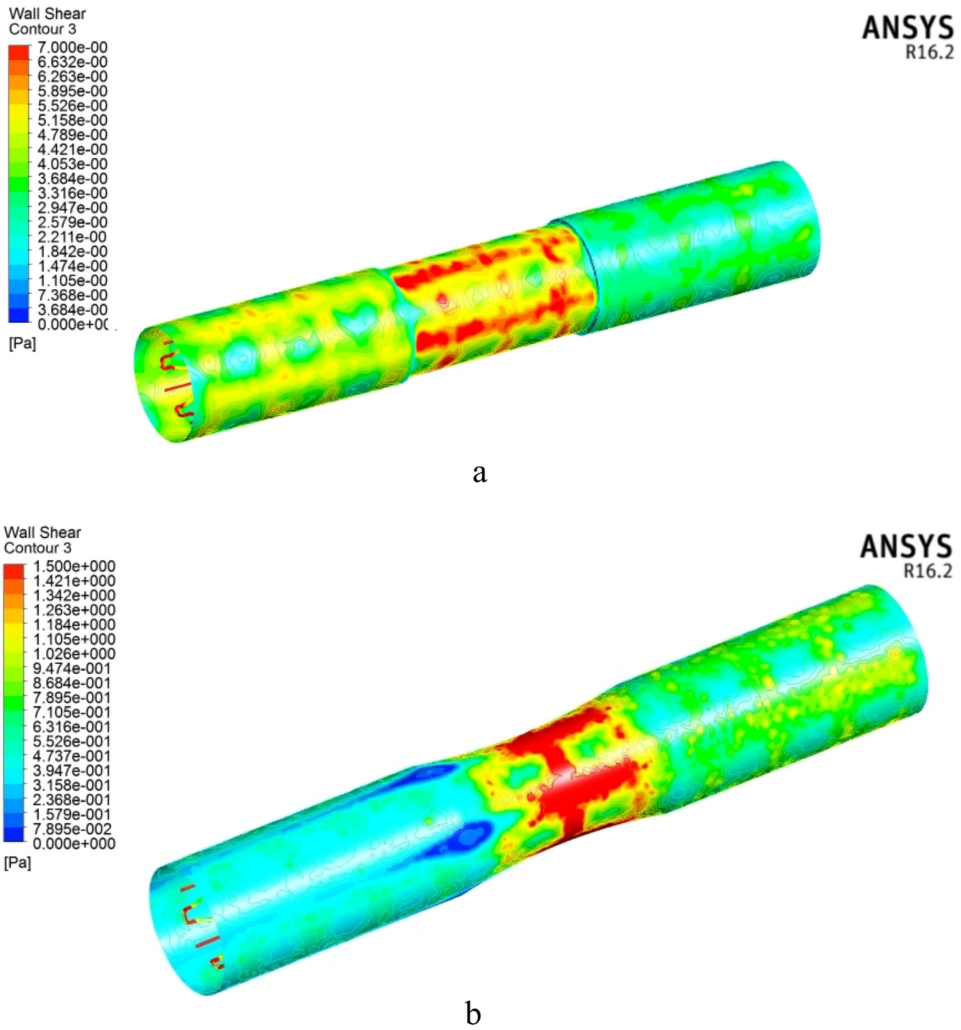


Fig. 9 Displays the effect of stent application on the shear stress distribution in the vessel **a** of cubic platelets and **b** of cylindrical platelets

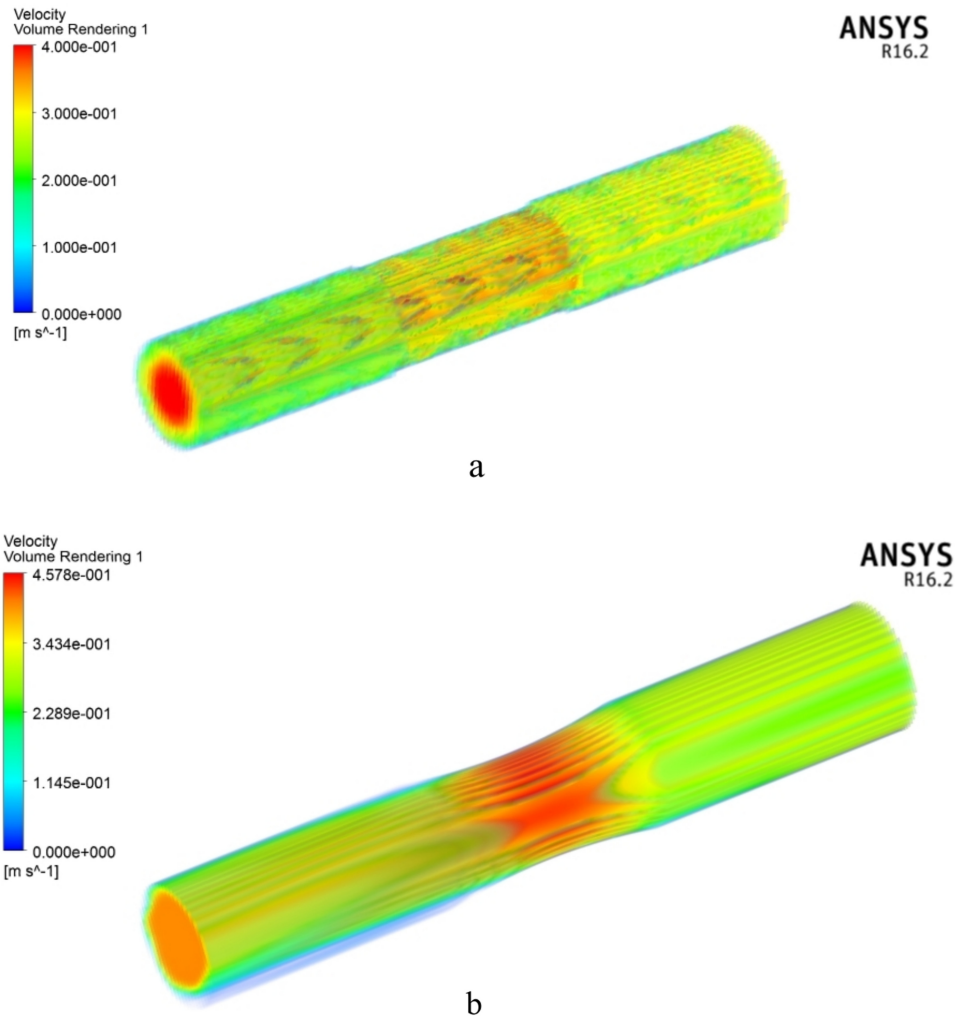


Fig. 10 Blood velocity distribution in a stent-bearing vessel in two states: **a** cube-shaped platelets and **b** cylindrical-shaped platelets

Author contributions Nan Tang: Writing—original draft preparation, conceptualization, supervision, project administration. Kangming Li: Methodology, software, validation, formal analysis. Haoran Li: Software, formal analysis, methodology, language review. Chunmei Qi: Formal analysis, methodology, software, language review.

Funding This work was supported by the Youth Medical Science and Technology Project of the Xuzhou Municipal Health Commission (Grant No. XWKYHT20210566).

Data availability The authors do not have permission to share data.

Declarations

Conflict of interest The authors declare no competing interests.

References

Akbar, N.S., Nadeem, S.: Carreau fluid model for blood flow through a tapered artery with a stenosis. Ain Shams Eng. J. **5**(4), 1307–1316 (2014)

Bahadori, F., Alizadeh, N., Hajyhosseinloo, M.: Investigation of stenosis effects on wall shear stress. Nashrieh Shimi va Mohandesi Shimi Iran **36**(3), 225–231 (2017)

Bai, H.G.: CFD simulation of density variation caused by anti-platelet drug in arteries affected by stenosis. Indian J. Sci. Technol. **8**(6), 562 (2015)

Bidel, Z., Hemati, R., Naserifar, R., Nazarzadeh, M., Del Pisheh, A.: Association of cardiovascular risk factors and coronary arteries involvement based on angiographic findings. J. Ilam Univ. Med. Sci. **22**(1), 147–154 (2014)

Bluestein, D., Einav, S., Slepian, M.J.: Device thrombogenicity emulation: a novel methodology for optimizing the thromboresistance of cardiovascular devices. J. Biomech. **46**(2), 338–344 (2013)

Cho, Y.I., Kensey, K.R.: Effects of the non-Newtonian viscosity of blood on flows in a diseased arterial vessel. Part 1: Steady flows. Biorheology **28**(3–4), 241–262 (1991)

Devi, C.U., Vijaya, R.B.: Study of Jeffrey fluid flow in an inclined tube with overlapping stenosis. Res. J. Sci. Technol. **9**(3), 400–404 (2017)

Durst, F.: Fluid Mechanics: An Introduction to the Theory of Fluid Flows. Springer, Berlin (2008)

El Kot, M., Abbas, W.: Numerical technique of blood flow through catheterized arteries with overlapping stenosis. Comput. Methods Biomech. Biomed. Eng. **20**(1), 45–58 (2017)

Eslami, G., Maleki, V.A., Rezaee, M.: Effect of open crack on vibration behavior of a fluid-conveying pipe embedded in a viscoelastic medium. Latin Am. J. Solids Struct. **13**, 136–154 (2016)

Fatholahi, M., Anvari, A., Akbari, O.A., Montazerifar, F., Ghaedamini, H., Toghraie, D., Nouraei, S.: Numerical investigation of mixed convection of nanofluid flow in oblique rectangular microchannels with nanofluid jet injection. Eur. Phys. J. Plus **136**(10), 1062 (2021)

Fraser, K.H., Zhang, T., Taskin, M.E., Griffith, B.P., Wu, Z.J.: A quantitative comparison of mechanical blood damage parameters in rotary ventricular assist devices: shear stress, exposure time and hemolysis index. J. Biomech. Eng. **134**(8), 56–78 (2012)

Gudino, E., Oishi, C.M., Sequeira, A.: Multiscale boundary conditions for non-Fickian diffusion applied to drug-eluting stents. SIAM J. Appl. Math. **77**(4), 1184–1203 (2017)

Hariharan, P., D'Souza, G., Horner, M., Malinauskas, R.A., Myers, M.R.: Verification benchmarks to assess the implementation of computational fluid dynamics based hemolysis prediction models. J. Biomech. Eng. **137**(9), 094501 (2015)

Husain, I., Labropulu, F., Langdon, C., Schwark, J.: A comparison of Newtonian and non-Newtonian models for pulsatile blood flow simulations. J. Mech. Behav. Mater. **21**(5–6), 147–153 (2013)

Kamada, H., Imai, Y., Nakamura, M., Ishikawa, T., Yamaguchi, T.: Shear-induced platelet aggregation and distribution of thrombogenesis at stenotic vessels. Microcirculation **24**(4), e12355 (2017)

Leng, X., Lan, L., Ip, V.H., Liu, H., Abrigo, J., Liebeskind, D.S., Wong, L.K., Leung, T.W.: Noninvasive fractional flow in intracranial atherosclerotic stenosis: reproducibility, limitations, and perspectives. J. Neurol. Sci. **381**, 150–152 (2017)

Li, X., Sun, B., Zhao, H., Ge, X., Liang, F., Li, X., Xu, J., Liu, X.: Retrospective study of hemodynamic changes before and after carotid stenosis formation by vessel surface repairing. Sci. Rep. **8**(1), 1–8 (2018)

Li, M., Walk, R., Roka-Moiia, Y., Sheriff, J., Bluestein, D., Barth, E.J., Slepian, M.J.: Circulatory loop design and components introduce artifacts impacting in vitro evaluation of ventricular assist device thrombogenicity: a call for caution. Artif. Organs **44**(6), E226–E237 (2020)

Liu, X., Du, Z., Han, T., Ghista, D.N., Lin, S., Wang, V., Wang, J., Zhang, H., Pan, Z.: Quantitative analysis of blood flow in cerebral venous sinus with stenosis by patient-specific CFD modeling. IEEE Access **7**, 3848–3854 (2018)

Long, Q., Merrifield, R., Xu, X., Kilner, P., Firmin, D., Yang, G.: Subject-specific computational simulation of left ventricular flow based on magnetic resonance imaging. Proc. Inst. Mech. Eng. [H] **222**(4), 475–485 (2008)

Maghami, E., Pejman, R., Najafi, A.R.: Fracture micromechanics of human dentin: a microscale numerical model. J. Mech. Behav. Biomed. Mater. **114**, 104171 (2021)

Malinauskas, R.A., Hariharan, P., Day, S.W., Herbertson, L.H., Buesen, M., Steinseifer, U., Aycock, K.I., Good, B.C., Deutsch, S., Manning, K.B.: FDA benchmark medical device flow models for CFD validation. ASAIO J. **63**(2), 150–160 (2017)

Mandal, P.K., Chakravarty, S., Mandal, A., Amin, N.: Effect of body acceleration on unsteady pulsatile flow of non-Newtonian fluid through a stenosed artery. Appl. Math. Comput. **189**(1), 766–779 (2007)

Moshfegh, A., Javadzadegan, A., Zhang, Z., Afrouzi, H.H., Omidi, M.: Effect of aortic spiral blood flow on wall shear stress in stenosed left main coronary arteries with varying take-off angle, stenosis severity and eccentricity. J. Mech. Sci. Technol. **32**(8), 4003–4011 (2018)

Nabavi, M., Nazarpour, V., Alibak, A.H., Bagherzadeh, A., Alizadeh, S.M.: Smart tracking of the influence of alumina nanoparticles on the thermal coefficient of nanosuspensions: application of LS-SVM methodology. Appl. Nanosci. **11**(7), 2113–2128 (2021a)

Nabavi, M., Elveny, M., Danshina, S.D., Behroyan, I., Babanezhad, M.: Velocity prediction of Cu/water nanofluid convective flow in a circular tube: Learning CFD data by differential evolution algorithm based fuzzy inference system (DEFIS). Int. Commun. Heat Mass Transf. **126**, 105373–74 (2021)

Nejad, A.A., Talebi, Z., Cheraghali, D., Shahbani-Zahiri, A., Norouzi, M.: Pulsatile flow of non-Newtonian blood fluid inside stenosed arteries: Investigating the effects of viscoelastic and elastic walls, arteriosclerosis, and polycythemia diseases. Comput. Methods Programs Biomed. **154**, 109–122 (2018)

Peskin, C.S.: Numerical analysis of blood flow in the heart. J. Comput. Phys. **25**(3), 220–252 (1977)

Prasad, K.M., Thulluri, S., Phanikumari, M.: Investigation of blood flow through an artery in the presence of overlapping stenosis. J. Nav. Archit. Mar. Eng. **14**(1), 39–46 (2017)

Rezaee, M., Arab Maleki, V.: Vibration analysis of a cracked pipe conveying fluid. Modares Mech. Eng. **12**(1), 66–76 (2012)

Rezaee, M., Arab Maleki, V.: Vibration analysis of fluid conveying viscoelastic pipes rested on non-uniform winkler elastic foundation. Modares Mech. Eng. **16**(12), 87–94 (2017)

Rezaee, M., Arab Maleki, V.: Passive vibration control of fluid conveying pipes using dynamic vibration absorber. Amirkabir J. Mech. Eng. **51**(3), 111–120 (2019)

Rezaee, M., Maleki, V.A.: An analytical solution for vibration analysis of carbon nanotube conveying viscose fluid embedded in viscoelastic medium. Proc. Inst. Mech. Eng. C J. Mech. Eng. Sci. **229**(4), 644–650 (2015)

Sadeqi, S., Rouhi, S., Xiros, N., Aktosun, E., VanZwieten, J., Sultan, C., Ioup, J.: Numerical investigation of an experimental ocean current turbine based on blade element momentum theory (BEM). In: International Conference on Offshore Mechanics and Arctic Engineering. American Society of Mechanical Engineers, New York (2021)

Skopalik, S., Hall Barrientos, P., Matthews, J., Radjenovic, A., Mark, P., Roditi, G., Paul, M.C.: Image-based computational fluid dynamics for estimating pressure drop and fractional flow reserve across iliac artery stenosis: a comparison with in-vivo measurements. Int. J. Numer. Methods Biomed. Eng. **37**(12), e3437 (2021)

Suzuki, H., Matsumoto, Y., Sugimura, K., Takahashi, J., Miyata, S., Fukumoto, Y., Taki, Y., Shimokawa, H.: Impacts of hippocampal blood flow on changes in left ventricular wall thickness in patients with chronic heart failure. Int. J. Cardiol. **310**, 103–107 (2020)

Taylor, C.A., Fonte, T.A., Min, J.K.: Computational fluid dynamics applied to cardiac computed tomography for noninvasive quantification of fractional flow reserve: scientific basis. J. Am. Coll. Cardiol. **61**(22), 2233–2241 (2013)

van Loon, R., Anderson, P.D., van de Vosse, F.N.: A fluid–structure interaction method with solid-rigid contact for heart valve dynamics. J. Comput. Phys. **217**(2), 806–823 (2006)

Vigmond, E.J., Clements, C., McQueen, D.M., Peskin, C.S.: Effect of bundle branch block on cardiac output: a whole heart simulation study. Prog. Biophys. Mol. Biol. **97**(2–3), 520–542 (2008)

Wells, R.G., Marvin, B.: Measuring SPECT myocardial blood flow at the University of Ottawa Heart Institute. J. Nucl. Cardiol. **28**(4), 1298–1303 (2021)

Zhang, D., Xu, P., Qiao, H., Liu, X., Luo, L., Huang, W., Zhang, H., Shi, C.: Carotid DSA based CFD simulation in assessing the patient with asymptomatic carotid stenosis: a preliminary study. Biomed. Eng. Online **17**(1), 1–12 (2018)

Zhao, Y.C., Vatankhah, P., Goh, T., Michelis, R., Kyanian, K., Zhang, Y., Li, Z., Ju, L.A.: Hemodynamic analysis for stenosis

microfluidic model of thrombosis with refined computational fluid dynamics simulation. Sci. Rep. **11**(1), 1–10 (2021)
Zhu, G., Yuan, W., Yuan, Q., Ge, Y., Yang, J.: Numerical investigation of the hemodynamic environment change in patient-specific intracranial aneurysm with progressive stenosis in unilateral internal carotid artery. Mol. Cell. Biomech. **16**, 55–76 (2019)

Publisher's Note Springer Nature remains neutral with regard to jurisdictional claims in published maps and institutional affiliations.

Springer Nature or its licensor (e.g. a society or other partner) holds exclusive rights to this article under a publishing agreement with the author(s) or other rightsholder(s); author self-archiving of the accepted manuscript version of this article is solely governed by the terms of such publishing agreement and applicable law.